BIOCHEMISTRY
including biophysical chemistry & molecular biology

ARTICLE

pubs.acs.org/biochemistry

Conformational Dynamics in a Truncated Epidermal Growth Factor Receptor Ectodomain

Noga Kozer,[†] Julie Rothacker,[‡] Antony W. Burgess,[‡] Edouard C. Nice,[‡,§] and Andrew H. A. Clayton*[,†]

[†]Centre for Micro-photonics, Faculty of Engineering and Industrial Sciences, Swinburne University of Technology, Victoria 3122, Australia

[‡]The Ludwig Institute for Cancer Research, Melbourne-Parkville Branch, P.O. Box 2008, Royal Melbourne Hospital, Victoria 3050, Australia

[§]Department of Biochemistry, Monash University, Clayton, Victoria 3080, Australia

Supporting Information

ABSTRACT: Structural studies have revealed two forms of the monomeric epidermal growth factor receptor (EGFR) ectodomain: a compact (tethered) form stabilized by interdomain interactions and an extended (untethered) form in the presence of ligand. An important question is whether the ligand induces a conformational transition from a tethered to untethered form or whether there is a preexisting conformational equilibrium between tethered and untethered states. To distinguish between these two possibilities, we investigated a truncated receptor, EGFR501 (spanning residues 1−501), that contains the minimal elements required for high-affinity ligand binding in solution. Conformational transitions and dynamics were inferred by means of fluorescence from five internal tryptophan residues that are located within or close to the ligand-binding domains of EGFR501. A preexisting conformational equilibrium between tethered and untethered states in EGFR501 was deduced from (1) the nonlinear Arrhenius temperature dependence of fluorescence and (2) fluorescence polarization showing independently mobile domains. In contrast, the ligand−EGFR501 complex revealed a linear Arrhenius temperature dependence of fluorescence and increased fluorescence polarization due to a lack of significant interdomain motions. The data suggest that the role of the ligand is to trap the EGFR501 in the untethered state that is transiently formed in solution through a preexisting conformational equilibrium.

The epidermal growth factor receptor (EGFR) is a member of the epidermal growth factor (EGF) receptor tyrosine kinase family.[1,2] The EGFR network contributes to a number of processes important to cancer development and progression, including cell proliferation, apoptosis, angiogenesis, and metastatic spread. EGFR overexpression and truncation[3] have been observed in a number of common cancers, including brain, lung, breast, colon, and prostate, giving credence to the notion that a molecular understanding of EGFR activation will yield clinical benefits. Signaling of the EGFR is generally thought to be initiated by ligand binding to the extracellular region, which leads to tyrosine kinase dimerization (oligomerization),[4] conformational rearrangements within a preformed oligomeric complex,[5] and further higher-order oligomeric transitions.[1,6]

The extracellular region of the EGFR contains four domains, designated domains I−IV. Domains I and III are β-helical ligand-binding domains. Domains II and IV are cystine-rich domains. Three-dimensional crystallographic data[7−10] as well as biophysical studies in solution[11] have identified two forms of the monomeric EGFR extracellular region: a compact (tethered) form stabilized by interdomain interactions and an extended (untethered) form in the presence of ligand. In the tethered (unliganded) form, interdomain interactions (a tether) between domains II and IV prevent exposure of the dimerization loop from domain II, thereby keeping the receptor in its monomeric state. This conformation also physically constrains ligand-binding domains I and III so they cannot simultaneously contact the ligand. In the untethered form (ligand-bound), the tether between domains II and IV is released, allowing simultaneous contact of the ligand by both domains I and III. This untethering also exposes a dimerization arm that allows interaction of the EGFR with itself or the other members of the erbB receptor family.

In principle, there are two ways in which the initially unliganded, tethered conformer is converted to the final liganded, untethered form. In the ligand-induced model, model 1, the tethered conformer (T) binds ligand (L) to form the liganded-tethered complex (TL). Subsequently, TL converts to the untethered liganded (UL) form via a conformational change:

$$T + L \rightarrow TL \rightarrow UL \qquad \text{(model 1)}$$

In the receptor-induced model (model 2), a minor population of the untethered receptor conformer (U) is in thermal equilibrium with the T conformer. Ligand binding to the U form shifts

Received: January 20, 2011
Revised: April 28, 2011
Published: May 18, 2011

Figure 1. Models of EGFR501 in tethered (A) and untethered (B) conformations. The polypeptide backbone is represented by the black ribbon. Tryptophan residues (red) are located in ligand-binding domains I and III and in the first module of domain IV (adjacent to domain III). Structures taken from the tethered full-length ectodomain (with residues 502−621 removed) (see ref 9) and the 2:2 EGFR−TGF-α complex (showing one monomer and no ligand) (see refs 6 and 7). Note the different orientation and separation between the tryptophan-containing domains in the tethered and untethered conformations.

the equilibrium to the final UL state:

$$T \leftrightarrow U + L \rightarrow UL \qquad \text{(model 2)}$$

Some experimental evidence exists for both models. Model 1 is supported by X-ray crystallographic structural studies, obtained at low pH, which have revealed a tethered, monomeric receptor with ligand bound to domain I (i.e., TL in model 1).[9] On the other hand, model 2 is supported by the observation of an unliganded, extended EGFR containing fluorescent probes at the termini (i.e., U in model 2).[12]

In this work, we have utilized fluorescence spectroscopy, a sensitive biophysical technique, to examine the conformational states and dynamics of EGFR in solution and at physiological pH. To provide a model system, we have chosen EGFR501 (residues 1−501), which contains the minimal elements required for high-affinity ligand binding (domains I−III and the first module of domain IV).[13] EGFR501 exhibits nanomolar affinity for EGF and TGF-α (10−40 nM)[13] and, in the crystal, adopts a conformation identical to that of the 2:2 full-length ectodomain EGF−EGFR complex.[7,8] Five tryptophans in EGFR501 are located within or close to the ligand-binding domains, which are not involved in direct contacts with ligand−receptor or receptor−receptor interfaces[7] (Figure 1). These tryptophans provide an intrinsic fluorescent probe of receptor structure obviating the need for chemical or genetically encoded probes.[14,15] Our studies were performed by monitoring the tryptophan fluorescence (quantum yield, wavelength position of emission spectrum, and fluorescence polarization) as a function of ligand, temperature, and denaturant. Our analysis of the temperature dependence of fluorescence and polarization reveals the presence of multiple conformers of EGFR501 and local motions of domains I and III in the absence of ligand but one detectable conformation in the EGFR501−EGF complex. We also followed the binding and denaturant-induced release of a fluorescently tagged EGF derivative. The results are compared with model 1 and model 2, and the implications for binding are discussed.

EXPERIMENTAL PROCEDURES

Materials. The preparation and purification of EGFR501,[13] EGFR621,[16] K35EGF,[1] and EGF-FITC[16] have been described previously. Guanidine hydrochloride (GuHCl, 98% pure) was from BDH Chemicals Ltd. The buffer was PBS containing 150 mM NaCl (pH 7.4).

Methods. *Instrumentation.* Tryptophan fluorescence and tryptophan fluorescence anisotropies were measured using a SPEX Fluorolog-tau2 spectrofluorometer operating in steady-state mode using procedures described in a previous publication.[17]

All measurements were taken at a controlled temperature using a circulating water bath. Temperatures were calibrated using a temperature probe inserted in a cuvette containing buffer. Unless otherwise specified, all measurements were taken at 20 °C.

Fluorescence Spectra. Tryptophan fluorescence spectra were recorded using 295 nm excitation and an emission range of 300−500 nm. The emission maxima were obtained from the wavelength at maximal intensity.

Relative Quantum Yield. The quantum yields of EGFR621, EGFR501, the EGFR501−K35EGF complex, and EGFR501 with 4 M GuHCl were measured relative to the quantum yield of EGFR501. Samples were created in PBS and adjusted to an optical density (OD) of <0.1 at the excitation wavelength (295 nm), and fluorescence spectra were recorded as described above. The quantum yield of the sample relative to the EGFR501 reference was determined from area under the fluorescence spectrum of EGFR501 and the sample with corrections for the fraction of light absorbed, using the equation

$$\mathrm{QY(relativetoEGFR501)} = [\mathrm{area(s)/area(r)}][(1-10^{-\mathrm{OD_r}})/(1-10^{-\mathrm{OD_s}})] \quad (1)$$

where QY(relative to EGFR501) is the quantum yield relative to EGFR501, area(s) and area(r) are the areas under the fluorescence spectra of the sample and EGFR501, respectively, and OD_r and OD_s are the optical densities (or absorbance) at 295 nm for EGFR501 and the sample, respectively.

Anisotropy Measurements. The polarized components of the fluorescence were measured in L-format under motorized polarizer control over a range of excitation wavelengths (305, 295, and 275 nm to excite tryptophan) and observed at an emission wavelength of 340 nm. The instrument correction factor (G) and anisotropy of the signal were obtained from the four permutations of the excitation and emission polarization directions (I_{vv}, I_{vh}, I_{hv}, and I_{hh}). The instrument correction factor was obtained from the intensities under horizontal-polarization excitation conditions ($G = I_{hv}/I_{hh}$). The fluorescence anisotropy (r) was calculated from the formula

$$r = (I_{vv} - GI_{vh})/(I_{vv} + 2GI_{hv}) \quad (2)$$

We also reported the fluorescence polarization to make a connection with previously published work. The fluorescence polarization (p) is defined by the equation

$$p = (I_{vv} - GI_{vh})/(I_{vv} + GI_{hv}) \quad (3)$$

Tryptophan fluorescence polarizations were measured by exciting tryptophan (in EGFR501 or EGFR621) with light at wavelengths of 295 or 305 nm, respectively (fluorescence observed at 340 nm), and the polarization ratio was obtained from the ratio of the two measured quantities [polarization ratio = $\rho = p(\mathrm{ex305})/p(\mathrm{ex295})$].

Data Analysis. *Ligand−Receptor Interaction Measured by Ligand (EGF-FITC) Fluorescence.* Anisotropy titrations using fluorescently tagged ligand (EGF-FITC) and EGFR501 were performed and analyzed as previously described.[16] For these measurements, the emission monochromator was removed to enhance signal detection. The fluorescein moiety was excited at 490 nm and the emission observed through a 520 nm cut-on filter to reject scattered light. The anisotropy of EGF-FITC was measured at a constant EGF-FITC concentration (3 nM) in the absence of EGFR501 and in the presence of increasing concentrations of EGFR501. The fluorescence anisotropy titration was fit to a 1:1 equilibrium binding model with a single dissociation constant (K_d). The total measured anisotropy (r) is the average anisotropy of the anisotropy of the free ligand (r_L) and the anisotropy of the ligand bound to receptor (r_{LR}) weighted by the concentrations of free (L) and bound ligand (LR)

$$r = (Lr_L + \mathrm{LR}r_{LR})/(L + \mathrm{LR}) \quad (4)$$

where the concentration of ligand receptor (LR) is related to the total concentration of added ligand (L_0) and receptor (R_0)

$$\mathrm{LR} = [(K_d + L_0 + R_0)/2] - [(K_d + L_0 + R_0)^2 - 4L_0R_0]^{0.5}/2$$

$$L = L_0 - \mathrm{LR} \quad (5)$$

The measured anisotropies (r) as a function of the concentration of EGFR501 (R_0) were fit using a least-squares analysis in Microsoft Excel. In the fitting, the FITC-EGF concentration (L_0) was fixed at 3 nM, the concentration of the receptor (R_0, EGFR501) was varied, the anisotropy of free ligand (r_L) was fixed at the measured value, and the anisotropy of ligand bound to receptor (r_{LR}) and the dissociation constant (K_d) were allowed to vary.

Ligand−Receptor Binding Stoichiometry Measured by EGFR501 Fluorescence. The reverse titration (constant receptor and variable ligand) employed the tryptophan fluorescence signal from EGFR501. To avoid interference from ligand fluorescence, we used an EGF derivative (K35EGF) devoid of tryptophan residues.[1] A change in the quantum yield of the receptor upon ligand binding was used to measure the interaction. The total fluorescence from EGFR501 (F) is given by the summation

$$F = (R \times \mathrm{QY_{free}} + \mathrm{LR} \times \mathrm{QY_{bound}})/(R + \mathrm{LR}) \quad (6)$$

where R and LR are defined above and the quantum yields of the free receptor (EGFR501) and bound receptor (EGFR501−K35EGF complex) are denoted by QY_{free} and QY_{bound}, respectively. In this case, $R = R_0 - RL$ and RL is given by eq 5.

For the case in which the EGFR501 concentration is more than 1 order of magnitude larger than the K_d (i.e., $R_0 \gg K_d$), the concentration of the EGFR501−K35EGF complex or LR, represented by eq 5, is no longer dependent on K_d. Instead, LR will increase linearly with added ligand until the receptor binding sites are filled. The concentration of the ligand at this point compared to that of the receptor reveals the stoichiometry of the complex. More explicitly, for the 1:1 stoichiometry case where $R_0 \gg K_d$, eq 6 becomes

$$F = [(R_0 - L_0)\mathrm{QY_{free}} + L_0\mathrm{QY_{bound}}]/R_0 = \mathrm{QY_{free}} + (L_0\mathrm{QY_{bound}})/R_0 \quad (7)$$

where R_0 is fixed, L_0, is increased, and the change in receptor (EGFR501) fluorescence as a function of added ligand is a linear function up to the point when all the EGFR501 is occupied with ligand. This point of saturation was estimated by linear forward extrapolation of the first two low receptor concentration points in the data and back linear extrapolation of the three highest concentration points in the data.

Analysis of Fluorescence Data as a Function of Temperature. The tryptophan fluorescence (from EGFR501, EGFR621, and the EGFR501−K35EGF complex) was measured as a function of temperature and analyzed in terms of either one or two conformational states. For two interconverting conformers, form A and form B (A ↔ B), the total fluorescence signal (F) as a

function of temperature, T, is given by the sum of the two conformers (F_A and F_B)

$$F(T) = F_A(T) + F_B(T) \quad (8)$$

The intensities of the conformer's fluorescence are determined by their equilibrium fractions and the (temperature-dependent) Arrhenius-type functions (which reflect the temperature dependencies of the fluorescence intensity of pure conformers)

$$F_A(T) = x_A \times \exp(b_A + m_A/T),$$
$$F_B(T) = x_B \times \exp(b_B + m_B/T) \quad (9)$$

where

$$x_A = 1/[1 + K(T)], \quad x_B = K(T)/[1 + K(T)] \quad (10)$$

and $K(T)$ is the temperature-dependent equilibrium constant for the equilibrium between the conformers (A ↔ B). Taking the natural (base e) logarithms of both sides of eq 9, we have the equation

$$\ln(F) = \ln(\{1/[1 + K(T)]\} \times \exp(m_A/T + b_A) + \{K(T)/[K(T) + 1] \times \exp(m_B/T + b_B)\}) \quad (11)$$

According to eq 11, the Arrhenius plot of fluorescence is linear for a single conformer (i.e., $K \rightarrow 0$) but nonlinear for two or more conformers. Arrhenius plots of the tryptophan fluorescence from EGFR501 and EGFR501 with ligand were first tested for linearity via regression analysis. Data from EGFR501 were fitted to eq 11 using least-squares analysis. The simplest model to describe the temperature dependence of the equilibrium constant was employed. This model is $K(T) = \exp[(-x + Ty)/T]$, where x and y are constants.

When the data set was fit, constraints on the parameter space were used, because of the large number of adjustable parameters. x, y, m_A, and b_B were varied in the analysis. Two different approaches were used to estimate the parameters describing the temperature dependence of fluorescence from conformer B. In the first approach, m_A was varied but linked to the value of m_B ($m_A = m_B$). B_B and B_A were allowed to vary, but the constraint $(m_B/T + b_B)/(m_A/T + b_A) < 2$ (at 298 K) was made on the basis that the observed change in the quantum yield of EGFR501 upon ligand binding was less than 50%. In the second approach, m_B and b_B were fixed to values obtained from the temperature dependence of the EGFR501−K35EGF complex. This assumption is rationalized on the basis of the fact that EGFR501 is in the untethered state in the presence of ligand.

Analysis of Anisotropy Data via Perrin Plot Analysis. A Perrin plot analysis of temperature-dependent anisotropy data was used to extract the limiting anisotropy (r_0) and hence the average rotational correlation time (ϕ) for tryptophan emission from EGFR501. Using the Perrin equation[18] (eq 12), the rotational correlation time (ϕ) and fluorophore rotational volume (V) may be determined from measurements of the steady-state anisotropy (r), given the lifetime (τ) and anisotropy in the absence of rotation (r_0).

$$1/r = 1/r_0 + \tau/\phi r_0 = 1/r_0 + (1/r_0)(1 + RT\tau/\eta V) \quad (12)$$

The intercept of the plot of the reciprocal of the anisotropy as a function of $T\tau/\eta$, the Perrin plot, yields the extrapolated anisotropy (apparent r_0). T was measured as described above; corresponding values of η were taken from the literature, and the lifetime as a function of temperature [$\tau(T)$] was estimated from the formula (proportionality of quantum yield with intensity and lifetime)

$$\tau(T) = [\tau(298\ \mathrm{K})F(T)]/F(298\ \mathrm{K}) \quad (13)$$

where F was defined previously and τ(298 K) is the fluorescence lifetime of EGFR501 at 298 K.

The fluorescence lifetime of EGFR501 or the EGFR501−K35EGF complex was not measured directly but estimated with the assumptions discussed below. Using the definitions

$$\mathrm{QY(EGFR621)} = k_r\langle\tau\rangle\mathrm{(EGFR621)},$$
$$\mathrm{QY(EGFR501)} = k_r\langle\tau\rangle\mathrm{(EGFR501)} \quad (14)$$

where QY is the quantum yield, $\langle\tau\rangle$ is the mean lifetime, and k_r is the average radiative rate. We made the assumption that the average radiative rate of the six tryptophans in EGFR621 would be similar to the average radiative rate of the five tryptophans in EGFR501, because the difference between EGFR501 and EGFR621 is the single tryptophan in domain IV. With this assumption

$$\langle\tau\rangle\mathrm{(EGFR501)} = \langle\tau\rangle\mathrm{(EGFR621)} \times \mathrm{QY(EGFR501)/QY(EGFR621)} \quad (15)$$

The calculated average value [$\langle\tau\rangle$(EGFR621) = 2.7 ns] for EGFR621[19] was used. The average lifetime was calculated from the published time-resolved fluorescence data in Table 3 of ref 19. The reported amplitudes (lifetimes) were 26.0 (0.58 ns), 39.6 (2.16 ns), and 34.4 (4.9 ns).[19]

RESULTS

Tryptophan Fluorescence from EGFR501. The X-ray structures of the EGFR501 ectodomain reveal the presence of tryptophan residues in domains I and III and in the first module of domain IV. These tryptophans form an integral part of the hydrophobic core of both ligand-binding domains and are somewhat shielded from solvent (Figure 1). As a consequence, the indole rings of two of the tryptophan residues in domain I and those in three of the tryptophan residues in domains III and IV are in the proximity of each other (i.e., <2 nm). To characterize the microenvironment of the tryptophan residues of EGFR501 in solution, we measured several properties of the tryptophan fluorescence. The wavelength of maximal emission was used as a probe of the micropolarity of the environment local to the indole rings of the tryptophan residues. The rotational diffusion of the tryptophan residues was measured from the emission anisotropy. A comparison between the emission polarization causing excitation at 295 nm with the corresponding quantity causing excitation at 305 nm was made to determine the average extent of resonance energy transfer between the tryptophan residues.[20−22] Energy migration is strongly dependent on the distance (inverse sixth power) and orientation between the indole rings of the tryptophan residues and is typically operative on the <1.5 nm scale for tryptophan. We used the polarization ratio as an indirect measure of the average integrity of the Trp−Trp interactions in the EGFR501 ectodomain.

Table 1 summarizes the properties of the EGFR501 ectodomain tryptophan fluorescence under various conditions (in the absence and presence of ligand or denaturant). In the absence of ligand or denaturant, the EGFR501 tryptophan fluorescence

Table 1. Summary of Tryptophan Fluorescence Parameters of the EGFR501 and EGFR621 Ectodomains in Solution and in the Presence of Ligand and/or Denaturant

	λ^a	p_{295}	p_{305}	ρ^b	$r_{305}{}^c$	QY^d
EGFR501	337	0.13	0.31	2.2	0.23	1.0
EGFR501−K35EGF	340	0.13	0.34	2.6	0.25	0.9
EGFR501 with 4 M GuHCl	355	0.11	0.16	1.5	0.11	0.5
EGFR621	336	0.15	0.32	2.1	0.24	0.7

[a] Wavelength of maximal fluorescence intensity in the emission spectrum (±1 nm). [b] Ratio of fluorescence polarizations being excited at 305 and 295 nm (±0.1 nm). [c] Fluorescence anisotropy being excited at 305 nm (±0.005 nm). [d] Quantum yield of the emission ratio (relative to free EGFR501) (±0.1).

spectrum was characterized by an emission maximum located at 337 nm. This value is blue-shifted relative to the value for water-exposed tryptophan residues (cf. the water-exposed tryptophan emission maximum at 350−355 nm) and indicates that the indole rings are in an environment somewhat shielded from solvent, consistent with their environment deduced from the X-ray structure. The tryptophan fluorescence polarization was found to depend on the excitation wavelength (Table 1). Excitation at the red edge of the absorption at 305 nm resulted in a fluorescence polarization that was 2.2-fold larger than the corresponding quantity with excitation at 295 nm (Table 1). The magnitude of the polarization ratio ($\rho = 2.2$) is indicative of the Weber red edge effect due to the migration of energy between proximal tryptophan residues.[20−22] In contrast, a polarization ratio of ≤1.5 would have indicated a lack of Trp−Trp interactions.[20−22] The presence of energy migration is also in good agreement with the X-ray structure model, showing two proximal tryptophans in domain I and three proximal tryptophans in domains III and IV.

The Tryptophan Fluorescence of the EGFR501 Ectodomain Is a Sensitive Probe of Receptor Conformational Changes. The wavelength positions of the emission maximum, fluorescence anisotropy, and relative fluorescence quantum yield were used as probes of the conformation of EGFR501 upon ligand binding and receptor unfolding. Titration curves are found in Figures 2 and 5 and discussed below.

An EGF analogue (K35EGF) lacking tryptophan residues but having full binding and biological activity was employed to examine the effect of ligand binding on the conformation of EGFR501.[1] Figure 2A shows the effect of adding increasing concentrations of K35EGF to a solution of EGFR501. As K35EGF is added, there is a linear decrease in the fluorescence from EGFR501 until the signal is saturated at an approximately 1:1 K35EGF:EGFR501 molar ratio (see also eqs 6 and 7 in Experimental Procedures). This is evidence that the tryptophan fluorescence from the ligand-bound conformation of EGFR501 is quenched relative to the tryptophan fluorescence from the unliganded conformation. The extent of fluorescence quenching upon addition of saturating amounts of K35EGF was measured at different EGFR501 concentrations (0.1, 1, and 10 μM) and found to differ by less than 5% (Figure 2B). This confirms that the quenching of tryptophan fluorescence of EGFR501 is predominantly due to a conformational change during formation of the EGFR501−K35EGF complex. A red shift in tryptophan emission, an increase in tryptophan fluorescence anisotropy, and an increase in the polarization ratio were also observed for EGFR501 upon addition of K35EGF (see Table 1). We attribute

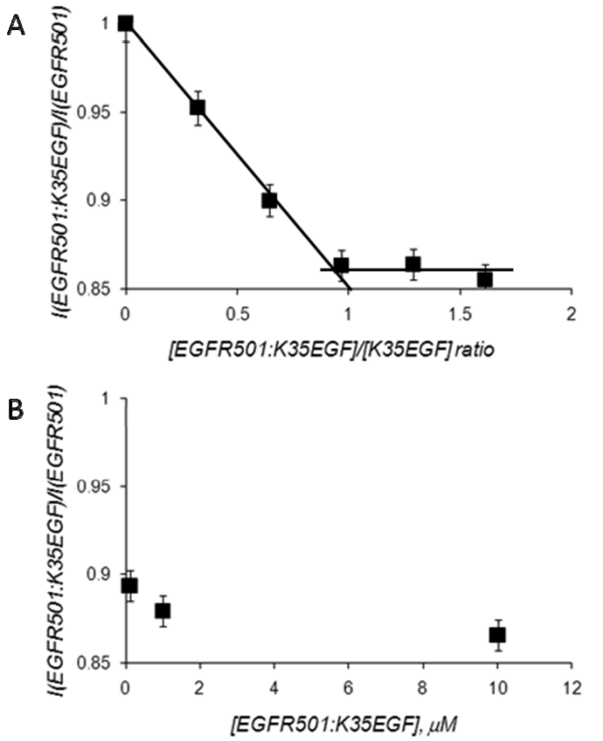

Figure 2. Conformational changes in the EGFR501 ectodomain studied using tryptophan fluorescence spectroscopy. (A) Binding of K35EGF ligand to EGFR501 from quenching of the intrinsic EGFR501 tryptophan fluorescence (EGFR501 concentration of 10 μM). Dots are the experimental data and solid lines the binding-curve extrapolations for a 1:1 K35EGF−EGFR501 interaction. (B) Fluorescence ratio between the EGFR501−K35EGF complex and EGFR501 as a function of the total EGFR501−K35EGF complex concentration (■).

the slight red shift of 3 ± 2 nm and the increase in the polarization ratio (increase of 10%) to a change in the environment of EGFR501 due to conformational transitions and K35EGF occupation. The increase in anisotropy indicates an increased level of restriction of rotational diffusion of the tryptophan residues and is discussed in more detail in the next section. Taken together, these observations provide evidence of a change in EGFR501 conformation and dynamics upon formation of the EGFR501−K35EGF complex. From the X-ray structure models (Figure 1), this conformational change involves a change in the orientation between domains I and III from the tethered T conformer to the liganded, untethered LU form.

To provide a point of reference, we compared the tryptophan fluorescence from EGFR501 in its native form to EGFR501 under denaturing conditions. Denaturation with 4 M GuHCl was shown to cause the greatest perturbation to EGFR501 structure as revealed by the large changes in tryptophan photophysical properties. As expected, unfolding at a high denaturant concentration resulted in complete exposure of the tryptophan residues to solvent (red shift in emission to 355 nm), a 50% reduction in quantum yield, an increase in the mobility of the tryptophan side chains (decrease in anisotropy), and a decrease in the separation between the tryptophan side chains [as reflected in the loss of energy migration and a decrease in the polarization ratio to 1.5 (see Table 1)]. These data suggest that, at this high concentration of GuHCl, the β-helical domains of EGFR501 are unfolded.

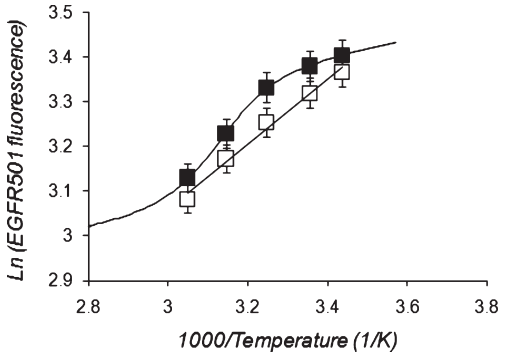

Figure 3. EGFR501 fluorescence as a function of temperature. Plot of the logarithm (base e, arbitrary units) of fluorescence (excitation at 295 nm, emission at 340 nm) of the EGFR501−K35EGF complex (□) and EGFR501 (■) as a function of reciprocal temperature (units of 1000/kelvin). The fit to the EGFR501−K35EGF complex fluorescence is linear [$R^2 = 0.99$ (solid line)]. The solid line associated with EGFR501 fluorescence is a fit to a temperature-dependent conformational transition model (see the text for details).

Conformational Transitions and Dynamics in EGFR501. The experiments described here show changes in EGFR501 conformation accompanying ligand binding. However, they do not allow us to determine whether the ligand induces a conformational transition from a T form to a U form (model 1) or whether there is a preexisting conformational equilibrium between T and U states (model 2). To determine whether EGFR501 is in a single tethered conformation (T) or in two conformations (tethered and untethered, T and U, respectively), we measured the fluorescence signal from EGFR501 as a function of temperature and plotted the resulting data in Arrhenius form. For proteins in a single global conformation, Arrhenius plots over a narrow temperature range are linear bur can become nonlinear when temperature-dependent conformational transitions occur.[23,24] Arrhenius plots for EGFR501 and EGFR501 in complex with K35EGF are shown in Figure 3.

The Arrhenius plot of the temperature dependence of the EGFR501 fluorescence signal was nonlinear in appearance and had a poor linear regression value ($R^2 = 0.94$). In contrast, the EGFR501−K35EGF complex fluorescence was linear, with an acceptable linear regression value [$R^2 = 0.99$; fit parameters $K \rightarrow \infty$, $m_B = 0.73$, and $b_B = 0.88$ (eq 11)]. This is evidence that EGFR501 can adopt two (or possibly more) conformations in the absence of ligand but only one conformation in the EGFR501−K35EGF complex.

The temperature-dependent fluorescence data from EGFR501 were fit a function that takes into account a temperature-dependent equilibrium between two conformers as well as the temperature dependencies of the fluorescence from each of the conformers (see eq 11 in Experimental Procedures). The data for the EGFR501 could be fit to eq 11 ($m_A = m_B = 0.2$; $b_A = 2.72$; $b_B = 2.46$) and the temperature-dependent equilibrium expression $K(T) = \exp[(-x + Ty)/T]$ [with varying parameters; $x =$ 15000, and $y = 47\ K^{-1}$ (see the solid line in Figure 3)]. We also employed a model in which m_A is not linked to the value of m_B and fixed the values of m_B and b_B to the values obtained from a linear fit of the temperature-dependent fluorescence data of the EGFR501−K35EGF complex (i.e., $m_B = 0.73$; $b_B = 0.88$; a values given above). The best-fit values to describe the temperature dependence of the equilibrium constant were $x = 14750$ and $y = 47\ K^{-1}$ for this model [SLS = 4×10^{-5} (data not shown)]. Both (two-conformer) models gave equally good fits to the EGFR501 data (SLS = $4-7 \times 10^{-5}$) and were significantly improved relative to the best fit to a single-conformer model (SLS = 2×10^{-3}).

According to both analysis approaches, at 298 K (25 °C), the conformational equilibrium is tilted toward the more stable conformer (probably the tethered conformation) with relative weight ranges of 90−98% A (T form) and 2−10% B (U form). We note that while the EGFR501 data set could be modeled using a temperature-dependent conformational transition model, the parameters extracted should perhaps be best considered as fitting parameters within the constraints imposed and not absolute thermodynamic quantities.

Model 1 and model 2 also predict different consequences for motional dynamics of EGFR501 and EGFR501−K35EGF complexes. In the preexisting T ↔ U conformational transition model (model 2), spontaneous thermally activated motions that alter the relative orientation of domain I with respect to domain III would be expected to decrease the overall rotational correlation time associated with the rotational motion of EGFR501, as compared to that of a rigid liganded UL conformer. Model 1 predicts the reverse situation: the rigid tethered conformation T is expected to be less flexible than the LT ↔ LU equilibrium.

To determine the rotational dynamics of the tryptophan residues in EGFR501 and the EGFR501−K35EGF complex, we analyzed the anisotropy data (Table 1) in terms of rotational correlation times. Using the Perrin equation[18] (see eq 12 in Experimental Procedures), the rotational correlation time (ϕ) was determined from measurements of the steady-state anisotropy (r), given the lifetime (τ) and anisotropy in the absence of rotation (r_0). To determine the limiting anisotropy in the absence of rotation (r_0), the temperature-dependent anisotropy and intensity of EGFR501 were recorded and analyzed according to Experimental Procedures. A representative Perrin plot for EGFR501 is shown in the Supporting Information. From the intercept of a linear regression, an extrapolated anisotropy (r_0) of 0.268 (excitation wavelength of 305 nm) was obtained. Using the extrapolated anisotropy, the measured steady-state anisotropy (Table 1), the estimated lifetime (eq 15), and eq 12 [$r = 0.23$, and $\tau = 3.8$ ns (see Experimental Procedures)], a rotational correlation time range, ϕ, of 21−26 ns (at 20 °C) was estimated for the average rotation of the tryptophan residues in EGFR501. The expected rotational correlation time for EGFR501 in the fixed (rigid) T conformation is expected to be 58 ns, as calculated from the EGFR501 structural model (Figure 1) using HYDROPRO (see ref 25). The shorter observed mean rotational correlation time of 21−26 ns therefore indicates the presence of tryptophan motions in smaller domains. This is evidence that instead of being constrained in a single tethered state (T conformer), the ligand-binding domains can sample different orientations in solution. For example, T to U transitions involve a large change in the orientation of domain III with respect to domain I; this change in orientation could decrease the tryptophan fluorescence anisotropy of EGFR501 with respect to a rigid conformation.

In the presence of K35EGF, the EGFR501 tryptophan anisotropy increased, indicating a decrease in the extent of domain motions in the EGFR501−K35EGF complex (see Table 1). A correlation time range of 48 ± 12 ns was computed from the Perrin equation (eq 12, eq 15, and Table 1 with an r_0 of 0.268, an r of 0.25, and a τ of 3.4 ns) for the EGFR501−K35EGF complex. This compares well with the theoretical rotational correlation

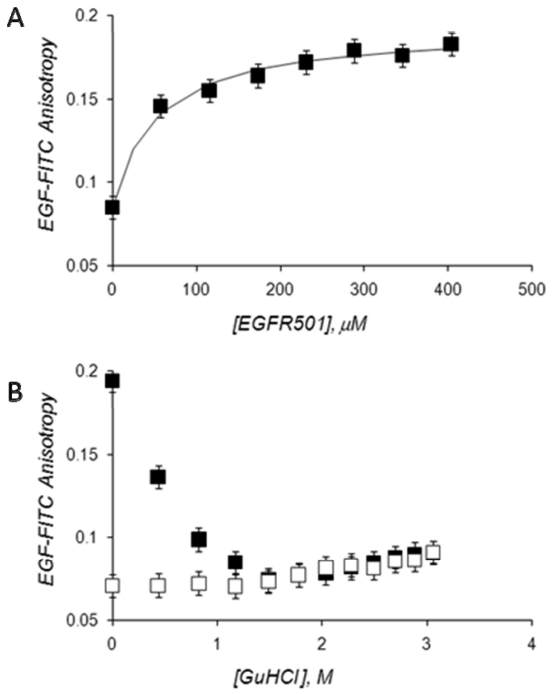

Figure 4. Binding and release of EGF-FITC with EGFR501 measured by ligand-labeled fluorescence anisotropy. (A) Plot of EGF-FITC anisotropy (3 nM) as a function of added EGFR501. The filled rectangles are the experimental data points, and the solid line is a fit to a ligand dissociation constant of 50 ± 20 nM. (B) Plot of free EGF-FITC (3 nM) anisotropy as a function of GuHCl concentration (□) and EGF-FITC in complex with EGFR501 [500 nM EGFR501 and 3 nM EGF-FITC (■)].

time for a rigid (i.e., fixed) untethered UL conformation of the EGFR501−EGF complex of 47 ns (again calculated from the structural model using HYDRPRO[25]). This suggests that the UL complex tumbles as a rigid entity. That is, there are no discernible transitions from TL to UL occurring on the nanosecond time scale.

In summary, the rotational correlation times for EGFR501 in the absence of ligand indicate rotational motions of tryptophan consistent with changes in the orientation of domain I with respect to domain III but in the presence of ligand indicate motion that would be more consistent with global tumbling of a single liganded UL complex. Taken together, with the temperature-dependent fluorescence data, these results are more consistent with model 2 than model 1 for EGFR501.

Partial Unfolding of EGFR501 but Not of Domains I and III Leads to Ligand Release. Our experiments revealed only one detectable conformation of the K35EGF−EGFR501 complex in solution, which is consistent with the UL conformation in model 2. However, the possibility remains that ligand can bind to domain I or III in a tethered TL conformation, inducing the transition to the untethered UL form, as in model 1, but the proportion of the TL intermediate is too small to detect in solution.

To test whether altering the orientation or separation between domains I and III causes ligand release, we conducted partial denaturation experiments using GuHCl and employing an EGF derivative (EGF-FITC) with a fluorescent tag attached as a probe of ligand-bound and ligand-free states.

We first determined conditions under which EGF was bound to EGFR501. Figure 4A shows the fluorescence anisotropy of an

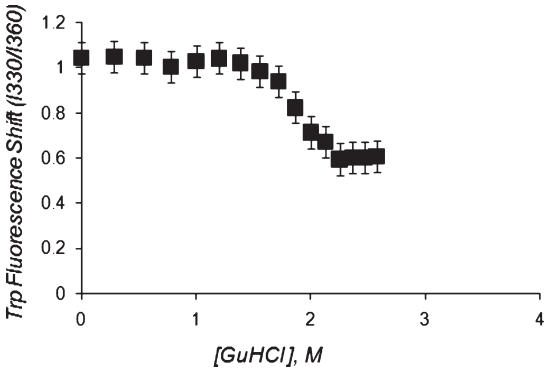

Figure 5. Denaturant-induced unfolding of EGFR501 measured by tryptophan fluorescence. Plot of the tryptophan fluorescence shift as a function of added GnHCl.

EGF-fluorescein conjugate (EGF-FITC ligand, fixed concentration of 3 nM) as a function of EGFR501 concentration. In the absence of EGFR501, the EGF-FITC fluorescence anisotropy is relatively low. As the concentration of EGFR501 is progressively increased, the anisotropy of EGF-FITC increases. This is evidence[16] of EGF-FITC (molecular mass of ∼6 kDa) binding to the larger EGFR501 (molecular mass of ∼66 kDa) molecule. Additional evidence comes from the magnitude of the dissociation constant estimated from this titration. The solid line in Figure 4A represents a theoretical fit to the data with a K_d of 50 ± 20 nM for the EGFR501−EGF-FITC interaction. The K_d value range of 30−70 nM is in reasonable agreement (i.e., within a factor of ∼2) with previous results (for TGF-α and EGF and EGFR501) obtained using SPR biosensor technology (10−40 nM).[13] The larger K_d values reported here might be, in part, due to the FITC probe.

To determine conditions of release of EGF-FITC from the EGFR501−EGF-FITC complex, we partially unfolded EGFR501 using low concentrations of the denaturant, GuHCl. Figure 4B shows the anisotropy of the EGF-FITC conjugate (3 nM) as a function of GuHCl for both the free ligand {EGF-FITC [Figure 4B (□)]} and in the presence of 500 nM EGFR501 [Figure 4B (■)]. As the GuHCl concentration is increased, the anisotropy of the EGFR501−EGF-FITC complex decreases and approaches that of (free) EGF-FITC. This indicates release of EGF-FITC from the EGFR501−EGF-FITC complex. The GuHCl concentration at half-release was 0.4 M. Note that this release is probably not due to denaturation of EGF, because this occurs with a midpoint of 3.9 M GuHCl.[26]

The results of the corresponding GuHCl denaturation experiments for the EGFR501 are shown in Figure 5. Because unfolding of domains I and III results in exposure of tryptophan residues to solvent and a corresponding red shift in the tryptophan fluorescence (Table 1), we used the ratio of fluorescence detected at 330 nm to the fluorescence detected at 360 nm as a measure of the extent of unfolding of β-helical domains I and III. In Figure 5, we have plotted this fluorescence ratio as a function of the concentration of GuHCl. Addition of GuHCl resulted in negligible (<10%) changes in the fluorescence ratio over the concentration range from 0 to 1 M and a red shift of EGFR501 tryptophan fluorescence over the GuHCl concentration range from 0 to 1.6 M with a denaturation midpoint of 1.9 M GuHCl. Taken together with the results described above, this suggests that β-helical domains I and III remain intact over the GuHCl

concentration range where EGF-FITC is released from EGFR501. This is evidence that partial unfolding of the EGFR501 ectodomain (probably domain II), but not ligand-binding domains I and III, causes release of ligand.

In the context of model 1 versus model 2, we interpret the denaturation experiments to imply that only the UL conformation with both domains I and III in contact with ligand can maintain a stable complex. This is consistent with model 2. In model 1, denaturation of domain II or IV could have released simultaneous contact of domains I and III with ligand, but the ligand−receptor complex would have remained intact though binding of either domain I or domain III to ligand, analogous with the process for TL in model 1. In this case, model 1 would have predicted denaturation behavior different from that observed; i.e., EGF-FITC would have dissociated concomitantly with denaturation of domain I or/and domain III (i.e., the midpoints of Figures 4B and 5 would have been identical).

Addition of the Second Module of Domain IV Stabilizes the Tethered Conformation. EGFR621 and EGFR501 differ by the extra 120 residues that make up the second module of domain IV. Addition of these extra residues is expected to add stabilization of the T (or TL) conformer relative to the U (or UL) conformer and consequently makes it more energetically costly to form the final UL state. In the context of model 1, this implies that the transition from TL to UL is energetically less favorable, but in the context of model 2, this implies that the transition from T to U is less favorable. The tryptophan fluorescence data from EGFR621 were consistent with stabilization of the T conformer. The Arrenhius plot of EGFR621 tryptophan fluorescence as a function of temperature was linear, consistent with the presence of only one detectable conformation over the temperature range investigated (see the Supporting Information). However, the anisotropy datum was inconsistent with a rigid tethered conformer T, because the average rotational correlation time for tryptophan motion was 23 ns (eq 12, eq 15, and Table 1 with an r_0 of 0.268, an r of 0.25, and a τ of 2.7 ns), which is much smaller than the rotational correlation time predicted for a protein of this size.

DISCUSSION

Our experiments were designed to answer an important question relevant to the first step in the activation of EGFR, the binding of ligand to receptor. How does the ligand influence a transition from a tethered T conformation to an untethered UL one? Does the ligand bind to a tethered intermediate TL, as in model 1? Does the ligand trap the receptor in an untethered conformation that preexists because of a conformational equilibrium of tethered and untethered (U ↔ T) states, as in model 2? To address these questions, we used the simplest model system capable of binding EGF with high affinity, EGFR501, and a sensitive biophysical technique suitable for detecting transitions and dynamics, fluorescence spectroscopy. Using a combination of fluorescence parameters, we have demonstrated that EGFR501 is not rigidly tethered but exists in several dynamically interconverting conformations in the absence of ligand. This is supported by two main lines of evidence. The first is the nonlinear Arrhenius plot of EGFR501 tryptophan fluorescence. This resembles similar behavior seen in the temperature-dependent fluorescence from two interconverting conformers of Syk kinase.[23] Second, the average rotational correlation time range for EGFR501 tryptophan motions (21−26 ns) is shorter than the correlation times predicted for global tumbling of either the T (55 ns) or U conformer (47 ns) but more consistent with segmental motions of domain I and/or domain III that convert T to U.

The change in tryptophan fluorescence upon ligand engagement indicates stabilization of the structure and dynamics of the ligand-binding domains of EGFR501. This is apparent from the increase in tryptophan fluorescence anisotropy and the linear Arrhenius fluorescence quenching profile observed for the EGFR501−K35EGF complex in solution. These spectroscopic measurements provide direct proof that ligand binding has locked the motions of the ligand-binding domains, consistent with the simultaneous contact of these domains with the ligand as observed in the X-ray models of the UL complex. In this respect, the ligand would appear to have a role in stabilization of a preexisting U conformation from an intrinsically dynamic structural ensemble as opposed to driving a conformational transition from one single rigid T conformation to another UL conformation.

The alternative model, model 1, the ligand-induced conformational change model, involves one unliganded conformation, T, and two liganded conformations, TL and UL. As discussed above, we have evidence of at least two conformational states in the absence of ligand, and we could detect only one conformational state in the presence of ligand through temperature perturbation. Attempts to trap an intermediate conformation with ligand still bound using partial denaturation also failed. Thus, for EGFR501 at least, the ligand-induced model is not supported by the spectroscopic evidence.

What are the implications for ligand binding? In model 2, for two interconverting receptor conformers, T and U, the apparent (i.e., measured) dissociation constant for the ligand−receptor interaction (K_d) is a function of the equilibrium constant for the receptor interconversion (K_{UT}), and the intrinsic equilibrium dissociation constant of the ligand in the receptor U conformer (K_{dU})

$$K_d = K_{dU}(1 + K_{UT}^{-1}) \quad (16)$$

Although a precise figure for K_{UT} cannot be given, our model-dependent analysis suggests that K_{UT} is in the range of 0.02−0.1 at 298 K. Given the measured (apparent) dissociation constant of 10−50 nM (this work and ref 13) in solution (K_d), this implies that the ligand dissociation constant (K_{dU}) in conformer U of EGFR501 is on the order of 0.2−5 nM.

The value for the dissociation constant deduced for the U conformer agrees reasonably well with the value obtained recently for a fluorescently tagged extended (U) EGFR621 derivative (5 nM).[12] The differences in the dissociation constants between the fluorescently tagged EGFR621 and U form EGFR501 might be due to the large (27 kDa) tags on fluorescent EGFR621, the approximations in the analysis used to derive K_{UT}, or both.

Our data and analysis are also consistent with recent attempts to detect untethered U EGFR forms of EGFR621. Lemmon's laboratory found that even when all the identified amino acids in the domain II−IV tether were mutated, EGFR621 still adopted a predominantly tethered configuration, as measured using X-ray scattering in solution.[11] EGFR501, which lacks the second module of domain IV, by necessity also lacks these key amino acids yet is also predominantly tethered T (>90%) according to our fluorescence analysis. However, according to model 2, only small differences in the U population translate into large

differences in overall binding affinity. For example, a K_d range from 20 to 200 nM can be ascribed to a fractional U population in the range of 0.5−5% (eq 16; K_{dU} = 1 nM). Thus might explain why amino acid mutations designed to untether EGFR621 affect ligand binding constants yet paradoxically do not appear to cause the appearance of detectable populations (by X-ray scattering) of U forms in the absence of ligand.[11] Clearly the assignment of conformational states can benefit from sensitive methods, like fluorescence spectroscopy, that can distinguish minor populations.

The work has utilized the simplest model system to examine aspects of conformational states of the EGFR. At the cell surface, the situation for the full-length EGFR is much more complex, with multiple conformational and oligomeric states and regulation by other effectors, such as membrane domains, and cytosolic interactions.[27] However, as we pointed out in previous work, the dissociation constant for the U form in solution appears to be remarkably close to the dissociation constants for the major low-affinity form of the EGFR expressed in cells.[12] If the correlation between conformation and affinity is correct, then this would imply that the EGFR is actually untethered on the cell surface. This is speculation that requires further examination. Our results also reveal that the monomeric U form of the EGFR ectodomain in solution does not have the affinity of the high-affinity binding sites for EGF on the surface of cells, so the high-affinity form must be regulated at another level.

Given the recent explosion in high-resolution structures of the major components of the EGFR, understanding the relationship between the fundamental biochemical events (ligand binding and tertiary and quaternary structural change) and receptor activation (and subsequent signaling) remains a fascinating topic of research inquiry for this archetypical type 1 receptor system.

■ ASSOCIATED CONTENT

Supporting Information. Temperature-dependent fluorescence anisotropy data for EGFR501 and temperature-dependent fluorescence data for EGFR621. This material is available free of charge via the Internet at http://pubs.acs.org.

■ AUTHOR INFORMATION

Corresponding Author

*Cell Biophysics Laboratory, Centre for Micro-Photonics, Faculty of Engineering and Industrial Sciences, P.O. Box 218, Hawthorn, Victoria 3122, Australia. Telephone: +61-3-92145719. Fax: +61-3-9214-5435. E-mail: aclayton@swin.edu.au.

Funding Sources

A.H.A.C. was partially supported by an R. D. Wright Biomedical Career Development Award from the Australian National Health and Medical Research Council (NHMRC). This work was also supported by NHMRC Grants 280918 and 433624 and funds from the Operational Infrastructure Support Program provided by the Victorian Government, Australia.

■ ABBREVIATIONS

EGF, epidermal growth factor; EGFR, epidermal growth factor receptor; EGFR501, residues 1−501 of the human EGFR ectodomain; EGFR621, whole human EGFR ectodomain (residues 1−621); GuHCl, guanidine hydrochloride; PBS, phosphate-buffered saline solution.

■ REFERENCES

(1) Clayton, A. H., Walker, F., Orchard, S. G., Henderson, C., Fuchs, D., Rothacker, J., Nice, E. C., and Burgess, A. W. (2005) Ligand-induced dimer-tetramer transition during the activation of the cell surface epidermal growth factor receptor-A multidimensional microscopy analysis. *J. Biol. Chem. 280*, 30392–30399.

(2) Lemmon, M. A., and Schlessinger, J. (2010) Cell signaling by receptor tyrosine kinases. *Cell 141*, 1117–1134.

(3) Yarden, Y., and Sliwkowski, M. X. (2001) Untangling the ErbB signalling network. *Nat. Rev. Mol. Cell Biol. 2*, 127–137.

(4) Yarden, Y., and Schlessinger, J. (1987) Self-phosphorylation of epidermal growth factor receptor: Evidence for a model of intermolecular allosteric activation. *Biochemistry 26*, 1434–1442.

(5) Gadella, T. W., Jr., and Jovin, T. M. (1995) Oligomerization of epidermal growth factor receptors on A431 cells studied by time-resolved fluorescence imaging microscopy. A stereochemical model for tyrosine kinase receptor activation. *J. Cell Biol. 129*, 1543–1558.

(6) Clayton, A. H., Orchard, S. G., Nice, E. C., Posner, R. G., and Burgess, A. W. (2008) Predominance of activated EGFR higher-order oligomers on the cell surface. *Growth Factors 26*, 316–324.

(7) Garrett, T. P., McKern, N. M., Lou, M., Elleman, T. C., Adams, T. E., Lovrecz, G. O., Zhu, H. J., Walker, F., Frenkel, M. J., Hoyne, P. A., Jorissen, R. N., Nice, E. C., Burgess, A. W., and Ward, C. W. (2002) Crystal structure of a truncated epidermal growth factor receptor extracellular domain bound to transforming growth factor α. *Cell 110*, 763–773.

(8) Ogiso, H., Ishitani, R., Nureki, O., Fukai, S., Yamanaka, M., Kim, J. H., Saito, K., Sakamoto, A., Inoue, M., Shirouzu, M., and Yokoyama, S. (2002) Crystal structure of the complex of human epidermal growth factor and receptor extracellular domains. *Cell 110*, 775–787.

(9) Ferguson, K. M., Berger, M. B., Mendrola, J. M., Cho, H. S., Leahy, D. J., and Lemmon, M. A. (2003) EGF activates its receptor by removing interactions that autoinhibit ectodomain dimerization. *Mol. Cell 11*, 507–517.

(10) Burgess, A. W., Cho, H. S., Eigenbrot, C., Ferguson, K. M., Garrett, T. P., Leahy, D. J., Lemmon, M. A., Sliwkowski, M. X., Ward, C. W., and Yokoyama, S. (2003) An open-and-shut case? Recent insights into the activation of EGF/ErbB receptors. *Mol. Cell 12*, 541–552.

(11) Dawson, J. P., Bu, Z., and Lemmon, M. A. (2007) Ligand-induced structural transitions in ErbB receptor extracellular domains. *Structure 15*, 942–954.

(12) Kozer, N., Henderson, C., Bailey, M. F., Rothacker, J., Nice, E. C., Burgess, A. W., and Clayton, A. H. (2010) Creation and biophysical characterization of a high-affinity, monomeric EGF receptor ectodomain using fluorescent proteins. *Biochemistry 49*, 7459–7466.

(13) Elleman, T. C., Domagala, T., McKern, N. M., Nerrie, M., Lonnqvist, B., Adams, T. E., Lewis, J., Lovrecz, G. O., Hoyne, P. A., Richards, K. M., Howlett, G. J., Rothacker, J., Jorissen, R. N., Lou, M., Garrett, T. P., Burgess, A. W., Nice, E. C., and Ward, C. W. (2001) Identification of a determinant of epidermal growth factor receptor ligand-binding specificity using a truncated, high-affinity form of the ectodomain. *Biochemistry 40*, 8930–8939.

(14) Pan, C. P., Muino, P. L., Barkley, M. D., and Callis, P. R. (2011) Correlation of Tryptophan Fluorescence Spectral Shifts and Lifetimes Arising Directly from Heterogeneous Environment. *J. Phys. Chem. B 115*, 3245–3253.

(15) Callis, P. R., Petrenko, A., Muino, P. L., and Tusell, J. R. (2007) Ab initio prediction of tryptophan fluorescence quenching by protein electric field enabled electron transfer. *J. Phys. Chem. B 111*, 10335–10339.

(16) Domagala, T., Konstantopoulos, N., Smyth, F., Jorissen, R. N., Fabri, L., Geleick, D., Lax, I., Schlessinger, J., Sawyer, W., Howlett, G. J., Burgess, A. W., and Nice, E. C. (2000) Stoichiometry, kinetic and binding analysis of the interaction between epidermal growth factor (EGF) and the extracellular domain of the EGF receptor. *Growth Factors 18*, 11–29.

(17) Clayton, A. H., and Sawyer, W. H. (1999) The structure and orientation of class-A amphipathic peptides on a phospholipid bilayer surface. *Eur. Biophys. J. 28*, 133–141.

(18) Weber, G. (1952) Polarization of the fluorescence of macromolecules. I. Theory and experimental method. *Biochem. J. 51*, 145–155.
(19) Greenfield, C., Hiles, I., Waterfield, M. D., Federwisch, M., Wollmer, A., Blundell, T. L., and McDonald, N. (1989) Epidermal growth factor binding induces a conformational change in the external domain of its receptor. *EMBO J. 8*, 4115–4123.
(20) Moens, P. D., Helms, M. K., and Jameson, D. M. (2004) Detection of tryptophan to tryptophan energy transfer in proteins. *Protein J. 23*, 79–83.
(21) Weber, G. (1960) Fluorescence-polarization spectrum and electronic-energy transfer in proteins. *Biochem. J. 75*, 345–352.
(22) Weber, G. (1960) Fluorescence-polarization spectrum and electronic-energy transfer in tyrosine, tryptophan and related compounds. *Biochem. J. 75*, 335–345.
(23) Grucza, R. A., Futterer, K., Chan, A. C., and Waksman, G. (1999) Thermodynamic study of the binding of the tandem-SH2 domain of the Syk kinase to a dually phosphorylated ITAM peptide: Evidence for two conformers. *Biochemistry 38*, 5024–5033.
(24) Bushueva, T. L., Busel, E. P., and Burstein, E. A. (1978) Relationship of thermal quenching of protein fluorescence to intramolecular structural mobility. *Biochim. Biophys. Acta 534*, 141–152.
(25) Garcia De La Torre, J., Huertas, M. L., and Carrasco, B. (2000) Calculation of hydrodynamic properties of globular proteins from their atomic-level structure. *Biophys. J. 78*, 719–730.
(26) Chang, J. Y., and Li, L. (2002) The disulfide structure of denatured epidermal growth factor: Preparation of scrambled disulfide isomers. *J. Protein Chem. 21*, 203–213.
(27) Mattoon, D., Klein, P., Lemmon, M. A., Lax, I., and Schlessinger, J. (2004) The tethered configuration of the EGF receptor extracellular domain exerts only a limited control of receptor function. *Proc. Natl. Acad. Sci. U.S.A. 101*, 923–928.